Photocatalytic degradation of methyl-red by immobilised nanoparticles of TiO_2 and ZnO

R. Comparelli*, P.D. Cozzoli*, M.L. Curri, A. Agostiano*,**, G. Mascolo*** and G. Lovecchio*****

* Dipartimento di Chimica, Università di Bari, via Orabona 4, I-70126, Bari, Italy (E-mail: *csilrc30@area.ba.cnr.it*; *csildc28@area.ba.cnr.it*; *agostiano@area.ba.cnr.it*)

** CNR IPCF – Bari Division c/o Dipartimento di Chimica, Università di Bari, via Orabona 4, I-70126 Bari, Italy (E-mail: *csilmc20@area.ba.cnr.it*)

*** Istituto di Ricerca Sulle Acque, Consiglio Nazionale delle Ricerche, Via F. De Blasio 5, I-70123 Bari, Italy (E-mail: *mascolo@area.ba.cnr.it; giangilov@libero.it*)

Abstract In this work, we report on the degradation of methyl-red (2-(4-Dimethylamino-phenylazo)-benzoic acid – C.I. 13020) under UV irradiation in the presence of nanosized ZnO and TiO_2. Oxide nanocrystals with controlled size were synthesised by using non-hydrolytic approaches and tested for the photocatalysed degradation. The performances of the immobilised nanoparticles were compared with their commercial counterparts after immobilization onto a solid support. The influence of some experimental conditions, namely pH and dye concentration, were investigated by monitoring the dye decoloration spectrophotometrically. Several intermediate by-products were identified by HPLC-MS, showing that two different mechanisms were operative during the photocatalytic oxidation.

Keywords Colloidal nanocrystals; degradation of organic pollutants; HPLC-MS; photocatalysis

Introduction

It is well established that semiconductor assisted-photodegradation of organic compounds represents a powerful tool to remove water pollutants. In order to circumvent difficulties associated with the photocatalyst recovery from the treated streams, a common approach has been based on the immobilization of the photocatalyst onto a suitable transparent support (e.g. quartz glass) (Neppolian *et al*., 2002; Guillard *et al*., 2002). In most cases, however, such an immobilization has resulted in a loss of degradation efficiency due to the consequent decrease of the active surface area. In this respect, nanosized semiconductor materials have been proved to be particularly effective for degrading contaminants under UV irradiation due to the increasing surface-to-volume ratio with decreasing nanocrystal size. Moreover, as the bandgap of nanostructured semiconductors depends on their dimension, the electron and hole redox potentials can be eventually tuned by modulating the size of the crystals.

In the present paper, highly crystalline, surfactant-capped ZnO and TiO_2 nanoparticles were synthesised by colloidal non-hydrolytic routes and immobilised onto a glass substrate to be tested as photocatalysts under UV irradiation. The degradation of a model pollutant (the organic dye methyl-red [2-(4-Dimethylamino-phenylazo)-benzoic acid) – C.I. 13020]) was followed to explore the potential of the catalytic system. The influence of pH and of the initial dye concentration was investigated with reference to their commercial counterparts. Several organic by-products were also identified by HPLC-MS. The results were encouraging as they indicated that immobilised nanosized ZnO and TiO_2 were catalytically active even in the presence of the organic-passivating layer at their surface.

Water Science and Technology **Vol 49 No 4 pp 183–188**

Methods

Chemicals. Commercial catalysts as TiO_2 "Degussa P25" (anatase 70%; surface area, 50 m^2g^{-1}; mean diameter, approximately 30 nm) and ZnO (particle diameter < 1 μm, mean diameter 200 nm, surface area 5 m^2g^{-1}) were purchased from Aldrich. Methyl-Red (2-(4-Dimethylamino-phenylazo)-benzoic acid), acetone, chloroform, heptadecane, titanium tetrachloride ($TiCl_4$), titanium isopropoxide ($Ti(OPr^i)_4$), zinc acetate ($ZnAc_2$), *t*-butylphosphonic acid (TBPA), tri-n-octylphosphine oxide (TOPO) were purchased from Aldrich. Hexadecylamine (HDA), dodecylamine (DDA), tri-n-octylamine (TOA), methanol, 2-propanol were purchased from Fluka. All aqueous solutions were prepared with doubly distilled water.

Procedures. Surfactant-capped ZnO (Cozzoli *et al*., 2003) and TiO_2 (Trentler *et al*., 1999) nanocrystals, both sizing about 7 nm, were synthesised according to earlier reported non-hydrolytic procedures. Briefly, ZnO nanocrystals were synthesised by thermal decomposition of $ZnAc_2$ in hot alkylamines (HDA, DDA or TOA) in the presence of TBPA as the size-regulating agent. TiO_2 nanocrystals were synthesised by reacting $TiCl_4$ with $Ti(OPr^i)_4$ at high temperature in heptadecane in the presence of TOPO as the stabilising agent. For both oxides, it was found that the metal precursor/stabiliser molar ratio was the key parameter that allowed us to easily modulate the nanoparticle mean size. Both ZnO and TiO_2 based photocatalytic devices were prepared using nanocrystals of about 7 nm, immobilised onto a glass substrate from a $CHCl_3$ solution by casting. The obtained ZnO and TiO_2 nanoparticles were characterised by spectroscopic (UV-vis absorption and photoluminescence) and structural (X-ray diffraction and transmission electron microscopy) techniques. ZnO (wurtzite) and TiO_2 (anatase) films, consisting of uniformly sized nanoparticles, were typically prepared by casting from nanocrystals dissolved in organic solvents after extraction from their surfactant reaction mixture; the same procedure was applied to the corresponding commercial oxide powders.

Methyl-red photodegradation. A typical experiment of dye degradation was performed in a quartz cell (1 cm width) in the presence of the oxide nanoparticles immobilised onto a transparent support. The methyl-red solution (3×10^{-5} M) was kept under stirring and irradiated by a high-pressure 200 W mercury lamp (λ>300 nm) under air. The system was arranged in a suitable geometry in order to monitor the reaction course *in situ*. The time course of the degradation reaction was investigated by evaluating the dye concentration decay as a function of illumination time: for this purpose, the evolution of methyl-red absorption spectrum was followed in the wavelength range between 250 and 600 nm. The pH of the dye solution was adjusted by proper addition of HCl or NaOH. At scheduled time intervals, an aliquot of the mixture was withdrawn for HPLC-MS analysis.

Analytical determinations. Absorption spectra of colloidal organic solutions of the extracted ZnO and TiO2 nanocrystals and of their thin films deposited onto transparent substrates were recorded by using a Cary 3 (Varian) spectrophotometer. The dye decoloration in aqueous solution under illumination was monitored by using an Ocean Optics UV-vis diode array spectrophotometer equipped with an optical fibre and a deuterium lamp. The dye concentration decay and the degradation by-products were identified by HPLC-UV-MS using a 1050-Ti chromatographic system (Agilent Technologies) equipped with a Ultimate UV detector (LC-Packing Dionex), set at 425 and 220 nm, interfaced to an API 165 mass spectrometer (Applied Biosystems/MSD Sciex) equipped with a turboionspray interface. The samples, injected by a Gilson 234 autosampler equipped with a 9010 Rheodyne valve and a 40 μl loop, were eluted at 0.4 ml/min through a Luna phenyl-hexyl

column (3 μm, 150 × 3 mm) and pre-column (Phenomenex) with the following gradient: from 5/25/70 (ammonium acetate 50 mM in methanol/methanol/water) to 5/75/20 in 10 min, which was then maintained for 5 min. The interface conditions were: nebulizer gas (air) = 1.2 L/min, curtain gas (nitrogen) =1 L/min, turboionspray gas (nitrogen at 300°C) = 6 L/min, needle voltage = 5,000 V, orifice voltage = 25 V and ring voltage = 200 V. The flow from the HPLC-UV was split to allow 200 μl/min to enter the turboionspray interface.

Results and discussion

Characterisation of the nanoparticles. Figure 1 shows the UV-vis absorption spectra of the prepared oxide nanoparticles. The nanocrystals were extracted from the reaction medium and re-dissolved in chloroform due to their surface organic coating. The wurtzite ZnO nanocrystals show the characteristic blue shift of the excitation absorption peak (Figure 1A) with decreasing particle size (for d< 10 nm), due to well-known quantum-confinement effects. The mean particle sizes of the nanocrystals were estimated by using the Debye–Scherrer formula.

Methyl-red degradation. The experimental data reported in Figure 2 show a progressive decrease of the absorbance maximum at 428 nm for both nanocrystalline ZnO and TiO_2 photocatalysed degradation of methyl-red under UV light. The fitting of absorbance maximum data vs. time indicates an exponential decay (see inset Figure 2). At a fixed illumination time, the percentage of the bleaching was proportional to the initial substrate content within the explored dye concentration range (data not reported). These evidences are in agreement with previously reported results which suggested a first-order kinetic, or a pseudo-first-order one (Gonçalves *et al*., 1999; Guangming *et al*., 1996).

In Figure 3 the decays of the quasi-molecular ion peak of methyl-red are shown as a function of illumination time for, (a) ZnO; and (b) TiO_2 catalysed reactions, respectively. Commercial ZnO powder was more effective in degrading the dye than its nanostructured counterpart (Figure 3a). The obtained results showed that the disappearance of methyl-red was slightly increased at low pH, being more pronounced for the ZnO nanocrystals. This can be reasonably explained by invoking the surface properties of the semiconductor, being dependent on pH, on surface hydroxyl groups and on adsorbed charged molecules (additives or intermediate by-products). At pH lower than the isoelectric pH value (pH_{ZPC}) (about 9 for ZnO), the ZnO nanoparticles' surface is positively charged, thus promoting the migration of photogenerated electrons from the interior of the nanocrystals to the surface and preventing electron-hole recombination processes. Although pH_{ZPC} for methyl-red is

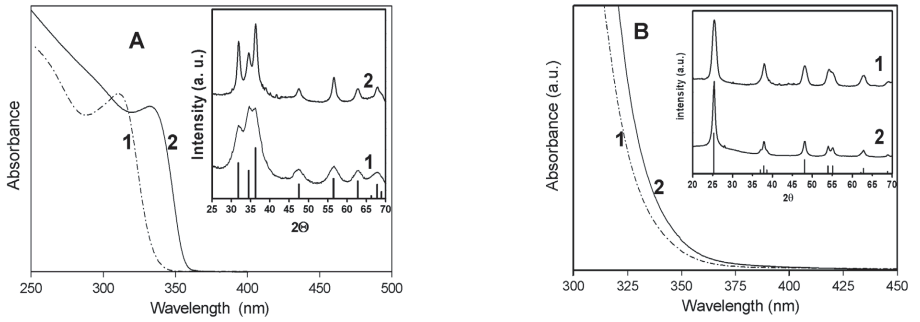

Figure 1 (A) UV-vis absorption spectra of: (1) 3.5 nm; and (2) 6.5 nm TBPA-capped ZnO nanoparticles in $CHCl_3$. (B) UV-vis absorption spectra of: (1) 6.5 nm; and (2) 12.5 nm TOPO-capped TiO_2 nanoparticles in $CHCl_3$. In the insets, the corresponding XRD patterns are reported. The average nanocrystal sizes were calculated by using Scherrer's formula

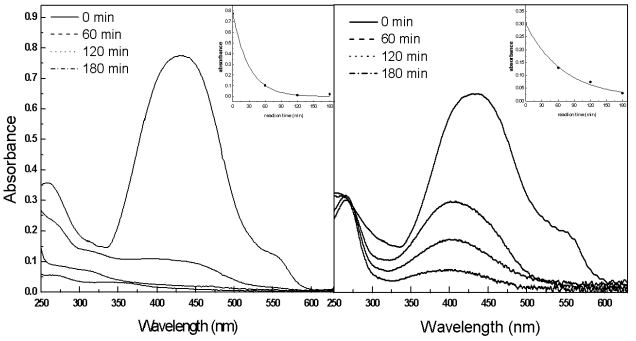

Figure 2 Spectrophotometric evaluation of the nanocrystalline TiO_2 (A) and ZnO (B) assisted photochemical degradation of methyl-red (pH = 6). In the corresponding insets (top right), the absorbance maximum at 428 nm is plotted vs. irradiation time

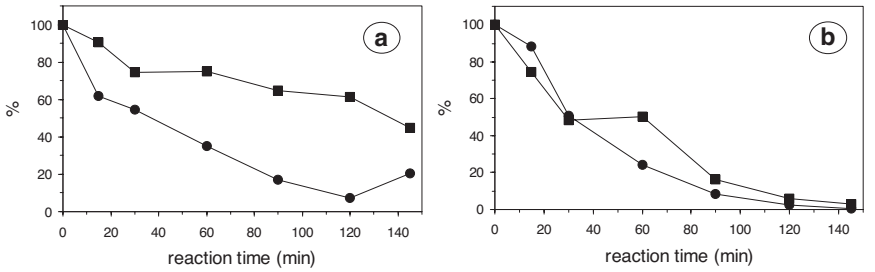

Figure 3 Methyl-red decays during photocatalytic degradation with immobilised ZnO (a) and TiO_2 particles (b). Initial methyl-red concentration = 3×10^{-5} M, pH = 6, semiconductors employed: commercial oxide (●), nanoparticles (■).

estimated to be 5.4, it was found that repulsive electrostatic interactions between the ZnO surface and charged dye molecules did not inhibit degradation to a considerable extent even at low pH values, as previously reported (Curri *et al.*, 2003).

In Figure 3b the decays of the dye in the presence of TiO_2 Degussa and of nanocrystalline TiO_2 show comparable results. At pH higher than pH_{ZPC} (5.1 for TiO_2), as the photogenerated electrons cannot easily overcome the negative charged surface, the holes may be prevented from reacting with the dye, thus ultimately recombining with the electrons. At pH values lower than TiO_2 pH_{ZPC}, the presence of surface hydroxyl groups as well as intermediate products (Al-Ekabi *et al.*, 1989) tightly adsorbed on TiO_2 nanoparticle surfaces, might be responsible for the inhibition of degradation. Finally, optimal reaction conditions were found at pH values near to TiO_2 pH_{ZPC}. At extreme pH values a repulsion effect can, in fact, occur due to the presence of homologous charges on the dye and on the catalyst.

The identification of some degradation by-products was carried out by HPLC-MS. The identified chemical structures of such by-products are reported in Table 1 and suggest that two main mechanisms of degradation can be active.

The first mechanism can involve the homolytic rupture of the bond between the amine nitrogen and methyl group possibly by means of direct photolysis. This route can also occur consecutively leading to by-product 1.

The second mechanism can involve the formation of hydroxyl radicals which originate from the oxidation of OH^- or H_2O by the photogenerated holes, or from the primary reactions of the photogenerated electrons with dissolved oxygen (Curri *et al.*, 2003; Al-Ekabi *et al.*, 1989; Zang *et al.*, 1995). The hydroxyl radicals can, in turn, attack the benzene rings of methyl-red leading to mono or polyhydroxylated by-products 3–6. These two mechanisms

Table 1 Proposed chemical structures, of some identified by-products ([M-H]$^+$ ions). For experimental conditions see text.

By product number	Chemical structure	[M-H]$^+$	TiO_2 commercial oxide	TiO_2 nanoparticles	ZnO commercial oxide	ZnO nanoparticles
1	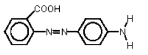	242	×	×		
2	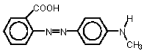	256	×	×	×	×
3	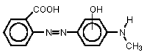	272			×	
4	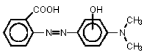	286	×	×	×	×
5	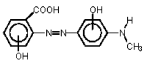	288		×		
6	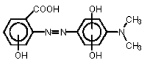	318	×	×		

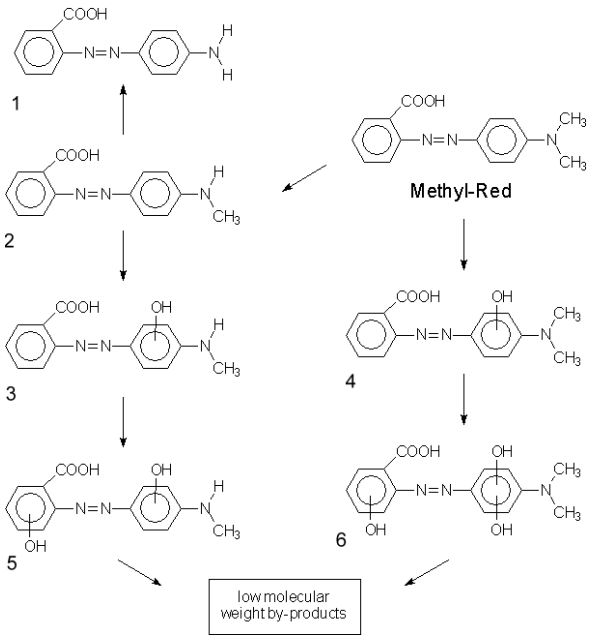

Figure 4 Proposed degradation pathway of methyl-red by immobilised TiO_2 and ZnO nanoparticles

could operate independently, as proven by the presence of by-products 3 and 5. Figure 4 depicts the proposed degradation pathway that takes into account the above reported degradation reactions.

Conclusions

ZnO and TiO_2 colloidal nanocrystals were successfully employed in thin film form for the photodegradation of methyl-red. The obtained results demonstrate a significant photocatalytic activity even in the presence of the organic capping layer on the nanocrystal surface. The higher efficiency of TiO_2 with respect to ZnO nanocrystals has been discussed on the basis of the surface chemistry of the nanoparticles. Several degradation by-products were identified by means of HPLC-MS, allowing us to propose a possible degradation pathway.

Detailed kinetics investigations are in progress in our laboratories to elucidate the kinetics of photodegradation processes in our systems.

References

Al-Ekabi, H., Serpone, N., Pelizzetti, E., Minero, C., Fox, M.A. and Draper, R.B. (1989). Kinetic studies in heterogeneous photocatalysis. 2. Titania-mediated degradation of 4-chlorophenol alone and in a three-component mixture of 4-chlorophenol, 2,4-dichlorophenol, and 2,4,5-trichlorophenol in air-equilibrated aqueous media. *Langmuir*, **5**, 250–255.

Cozzoli, P.D., Curri, M.L., Agostiano, A., Leo, G. and Lomascolo, M. (2003). Synthesis and characterisation of ZnO nanocrystals by a novel non-hydrolytic route. *J. Phys. Chem. B*, **107**(20), 4756–4762.

Curri, M.L., Comparelli, R., Cozzoli, P.D., Mascolo, G. and Agostiano, A. (2003). Colloidal oxide nanoparticles for the photocatalytic degradation of organic dye. *Mat. Sci. Eng. C*, **23**, 285–289.

Gonçalves, M.S.T., Oliveira-Campos, A.M.F., Pinto, E.M.M.S., Plasência, P.M.S. and Queiroz, M.J.R.P. (1999). Photochemical treatment of solutions of azo dyes containing TiO_2. *Chemosphere*, **39**(5), 781–786.

Guangming, L., Taixing, W., Jincai, Z., Hisao, H. and Serpone, N. (1999). Photoassisted degradation of dye pollutants. 8. Irreversible degradation of alizarin red under visible light radiation in air-equilibrated aqueous TiO_2 dispersions. *Environ. Sci. Technol.*, **33**, 2081–2087.

Guillard, C., Beaugiraud, B., Dutriez, C., Herrmann, J.-M, Jaffrezic, H., Jaffrezic-Renault, N. and Lacroix, M. (2002). Physicochemical properties and photocatalytic activities of TiO_2 films prepared by sol-gel methods. *Appl. Cat. B*, **39**(4), 331–342.

Neppolian, B., Choi, H.C., Sakthivel, S., Banumathi, A. and Murugesan, V. (2002). Solar/UV-induced photocatalytic degradation of three commercial textile dyes. *J. Haz. Mat.*, **89**, 303–317.

Trentler, T.J., Denler, T.E., Bertone, J.F., Agrawal, A. and Colvin, V.L. (1999). Synthesis of TiO_2 nanocrystals by nonhydrolytic solution-based reactions. *J. Am. Chem. Soc.*, **121**(7), 1613–1614.

Zang, L., Liu, C.-Y. and Ren, X.-M. (1995). Photochemistry of semiconductor particles. *J. Chem. Soc. Faraday Trans.*, **91**(5), 917–923 (see references cited therein).